The quantum perturbed cat map and symmetry

2005 J. Phys. A: Math. Gen. 38 5895

(http://iopscience.iop.org/0305-4470/38/26/005)

INSTITUTE OF PHYSICS PUBLISHING JOURNAL OF PHYSICS A: MATHEMATICAL AND GENERAL

J. Phys. A: Math. Gen. **38** (2005) 5895–5912 doi:10.1088/0305-4470/38/26/005

The quantum perturbed cat map and symmetry

M Degli Esposti and B Winn[1]

Dipartimento di Matematica, Università di Bologna, 40127 Bologna, Italy

E-mail: desposti@dm.unibo.it and brian.winn@math.tamu.edu

Received 8 April 2005, in final form 17 May 2005
Published 15 June 2005
Online at stacks.iop.org/JPhysA/38/5895

Abstract

We investigate a class of quantum symmetries of the perturbed cat map which exist only for a subset of possible values of Planck's constant. The effect of these symmetries is to change the spectral statistics along this positive-density subset. The symmetries are shown to be related to some simple classical symmetries of the map.

PACS numbers: 05.45.Mt, 03.65.−w
Mathematics Subject Classification: 81Q50, 81S05

1. Introduction

It has been recognized that quantum maps represent a useful model for the investigation of spectral properties of quantum systems with a chaotic classical limit. It is believed that in such systems the chaotic nature of the dynamics leaves a 'fingerprint' on the quantum spectrum in the form of correlations. This is in contrast to systems with an integrable dynamical system at the classical limit, for which the quantum energy levels are expected to be uncorrelated [6]. In the chaotic case, the correlations are expected to be the same as those in the eigenvalues of large random matrices [8, 9] with the same symmetries as the system under consideration. This behaviour is *universal* in the sense that it appears to be true for large classes of very diverse chaotic (mostly hyperbolic) systems. It has been observed numerically, and in part analytically, for chaotic billiards, geodesic flow on compact surfaces with negative curvature, quantum graphs and quantum maps, with a small number of non-generic exceptions (such as systems with strong arithmetical properties) [3, 7, 17, 20, 23].

This universal behaviour permits the study of systems that can be physically quite unusual, such as quantum maps, in order to gain a clearer understanding of more physically relevant systems. A quantum map is a quantum counterpart of an area-preserving map on the 2-torus which is viewed as a phase space. Examples, references and a detailed review of the relevant theory are given in [12]. A quantum map is a unitary operator acting on an N-dimensional state

[1] Present address: Department of Mathematics, Texas A&M University, College Station, TX 77843-3368, USA.

space, where the compact phase space restricts the allowed values of Planck's constant to be of the form $\hbar = (2\pi N)^{-1}$ for $N \in \mathbb{N}$. This operator is also sometimes called the propagator, and it can be represented in a suitable basis as an $N \times N$ matrix. The most famous examples are the hyperbolic automorphisms, which were also the subject of the first study of quantum maps [19]. They are (more or less) popularly known as cat maps, and the quantum version as quantum cat maps. They form the basis of the model in the present paper.

Returning, for a moment, to generalities for a quantization of a chaotic map, the random matrix hypothesis suggests that correlations in the spectrum of eigenvalues should mirror those of the appropriate ensembles of unitary matrices, the so-called circular ensembles[2] [26]. Following the work of Berry and Robnik [5, 29], the following picture emerged. Given a quantum map with propagator U, if there exists an antiunitary transformation W satisfying $WUW^{-1} = U^{-1}$, then W is said to be an antiunitary symmetry of U. In this case, there is a basis in which U is symmetric, so one expects the correlations in the spectrum to be the same as those of the circular orthogonal ensemble (COE) of symmetric unitary matrices. To be mathematically precise, one can conjecture that in the limit $N \to \infty$ statistics of a fixed, finite, number of eigenvalues converge to those of matrices from the COE averaged over the ensemble. (We describe one such indicator of correlations in spectra, the nearest-neighbour distribution, in appendix A.) If no such W exists then we consider in place of the COE, the circular unitary ensemble (CUE) of unrestricted unitary matrices. In fact, the CUE coincides with the probability space formed by the compact group $U(N)$ taken with normalized Haar measure.

A typical example of antiunitary symmetry is quantized time reversal (which classically maps the torus point (q, p) to $(q, -p)$). This is nothing more than complex conjugation, which is easily seen to be antiunitary. But even in systems with broken time-reversal symmetry, provided there exists some other antiunitary symmetry, the spectral statistics will still be those of the COE. A prominent example of this 'false T breaking' occurs in Aharonov–Bohm billiards for certain parameter values [5].

The random matrix conjectures above presuppose that the maps possess no other relevant symmetries, which would be other non-trivial unitary operators commuting with U. Verifying that this is the case can be a difficult task. Usually, each symmetry of the quantum propagator corresponds to a quantization of a classical symmetry of the map. However, it is now understood that in the case of (unperturbed) cat maps there is, for fixed N, a large collection of non-trivial matrices that commute with the quantum propagator U [21, 24]. These symmetries are tricky to handle because they do not have a classical limit; they are not related to any classical symmetry of the system and are called pseudo-symmetries or Hecke operators. The presence of a large number of symmetries is responsible for the strong failure of the random matrix conjecture in these models.

Under certain circumstances, small non-linear perturbations of the cat maps can be quantized, and the perturbations are sufficient to break the pseudo-symmetries. That is to say that these extra symmetries possessed by the unperturbed propagator are not present in the perturbed propagator, and the quantum spectrum becomes of random matrix type. But it is known that this does not always happen. If the perturbation is badly chosen, some of the pseudo-symmetries can survive perturbation. This has a number of consequences. The most striking is in the case where a perturbation is chosen that breaks time-reversal symmetry of the map. If the perturbation leaves intact an antiunitary *pseudo-symmetry*, then the quantum map has a antiunitary symmetry that is not obvious from the classical symmetries. The spectrum will look like the COE, when one would rather expect it to be typical of the CUE if only

[2] Probability spaces of matrices are referred to as *ensembles*.

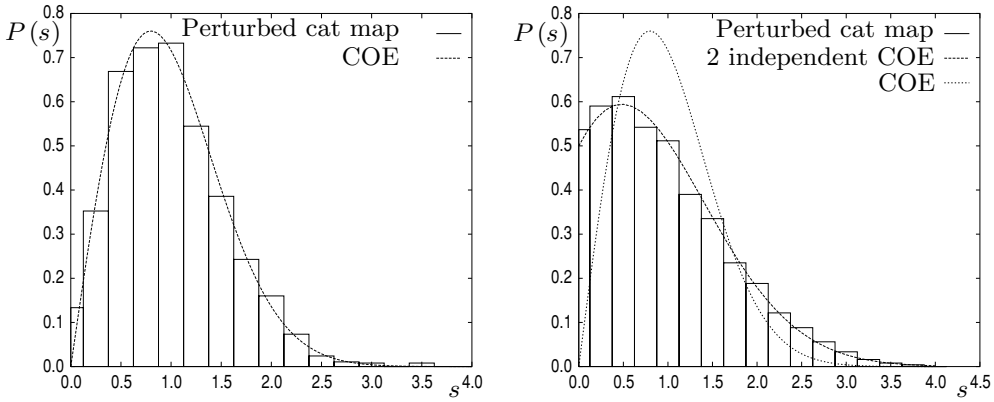

Figure 1. The nearest-neighbour spacing distribution for the quantum propagator of the map (1) (boxes) with $\kappa = 0.01$, for $N = 2998$ (left) and $N = 2996$ (right). The curves are the nearest-neighbour spacing densities for the COE and for a superposition of two independent COE spectra (right plot only).

classical symmetries were taken into account [21]. Thus, it is impossible to decide to which universality class a given system belongs, based only on knowledge of its classical symmetries.

In this paper, we report on a class of quantum symmetries of non-linear shear-perturbed quantum cat maps which exist only for certain values (a positive-density subset) of N. The effect of these symmetries is to change the spectral statistics of the map for these values of N. As we will see, these symmetries have a very natural classical interpretation, and they are different from the Hecke symmetries previously discussed. Not all of the symmetries we construct are new; some were previously noted in [21] although with the emphasis on using them to build antiunitary symmetries. In the present work, we develop their properties and effects on spectral statistics in more detail. Another recent example of a quantum map whose spectral statistics depend strongly on the choice of N was given in [18].

Our investigation was motivated by the following numerical experiments. Figure 1 shows two simulations of nearest-neighbour spacing distribution (see appendix A) for the eigenvalues of the quantum propagator of the map

$$\begin{pmatrix} q \\ p \end{pmatrix} \mapsto \begin{pmatrix} 6 & 5 \\ 7 & 6 \end{pmatrix} \begin{pmatrix} q \\ p \end{pmatrix} + \frac{\kappa}{2\pi} \begin{pmatrix} 5 \\ 6 \end{pmatrix} \cos(2\pi q) \mod 1. \tag{1}$$

The map (1) is a shear perturbation of a cat map (see below for the details of the quantization). This map has time-reversal symmetry, and hence an antiunitary symmetry, so according to the random matrix conjecture we expect that the spacing distribution of eigenangles of the propagator will converge to that of the COE as $N \to \infty$. For $N = 2998$ we see good agreement with the COE curve, but for $N = 2996$ we see that the distribution is very far from that of the COE. In fact, it appears to be very close to the distribution of a superposition of two independent COE spectra.

In figure 2 is shown the nearest-neighbour spacing distribution for $N = 3006$ and $N = 3008$ for the map

$$\begin{pmatrix} q \\ p \end{pmatrix} \mapsto \begin{pmatrix} 4 & 9 \\ 7 & 16 \end{pmatrix} \begin{pmatrix} q \\ p \end{pmatrix} + \frac{\kappa}{2\pi} \begin{pmatrix} 4 \\ 7 \end{pmatrix} \cos(2\pi p) + \frac{\kappa}{2\pi} \begin{pmatrix} 9 \\ 16 \end{pmatrix} \cos(2\pi q + \kappa \cos(2\pi p)) \mod 1. \tag{2}$$

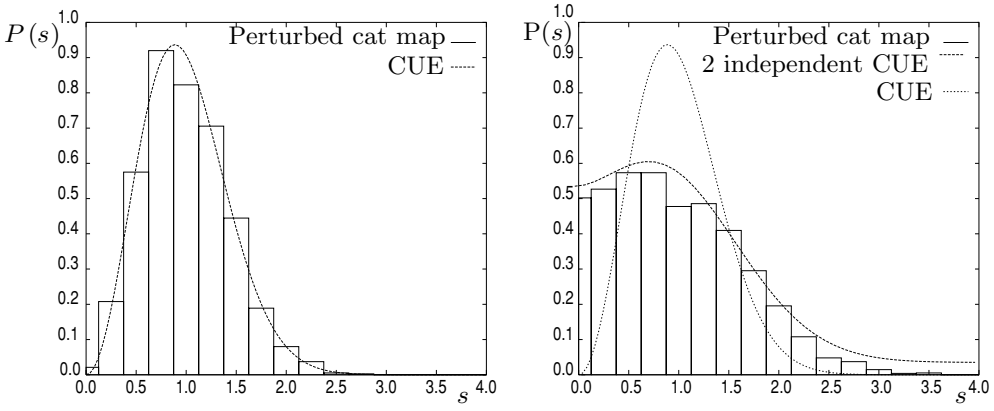

Figure 2. The nearest-neighbour spacing distribution for the quantum propagator of the map (2) (boxes) with $\kappa = 0.01$, for $N = 3006$ (left) and $N = 3008$ (right). The curves are the nearest-neighbour spacing densities for the CUE and for a superposition of two independent CUE spectra (right plot only).

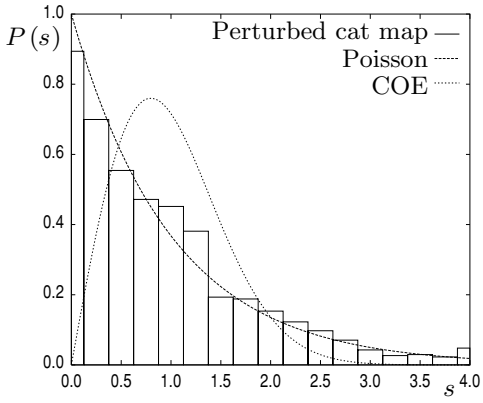

Figure 3. The nearest-neighbour spacing distribution for the quantum propagator of the map (3) (boxes) with $\kappa = 0.01$, for $N = 3003$. The curves are the nearest-neighbour spacing densities for a Poisson (uncorrelated) process and for the COE.

This more complicated map is a composition of a cat map with two shears, and was chosen as an example without antiunitary symmetry [21], so one would expect to see CUE statistics. For $N = 3006$ the agreement is good, but for $N = 3008$ the distribution appears closer to that of a superposition of two CUE spectra.

The final numerical picture that we seek to explain is given in figure 3 which shows the nearest-neighbour spacing distribution for $N = 3003$ for the map

$$\begin{pmatrix} q \\ p \end{pmatrix} \mapsto \begin{pmatrix} 12 & 13 \\ 13 & 14 \end{pmatrix} \begin{pmatrix} q \\ p \end{pmatrix} + \frac{\kappa}{2\pi} \begin{pmatrix} 13 \\ 14 \end{pmatrix} \cos(2\pi q) \mod 1. \tag{3}$$

As with the map (1), this map has time-reversal symmetry, so one should compare with the statistics of the COE. However, from the plot, the actual distribution of spacings appears to be somewhat closer to the level spacing distribution of events from a Poisson process, which is

the conjectured level spacing distribution for classically integrable (so strongly non-chaotic) dynamical systems [6].

In section 3, we offer explanations for the numerics observed in these figures.

2. The model and results

The first quantization of a map was given by Hannay and Berry [19] who considered the linear map $A : \mathbb{T}^2 \to \mathbb{T}^2$ defined by

$$A\begin{pmatrix} q \\ p \end{pmatrix} := \begin{pmatrix} A_{11} & A_{12} \\ A_{21} & A_{22} \end{pmatrix}\begin{pmatrix} q \\ p \end{pmatrix} \mod 1. \tag{4}$$

As usual, we abuse notation by referring to A both as the map on the torus and the 2×2 matrix which represents it. In order to preserve continuity and area, the elements of A should be integers and the determinant should be unity. The dynamics of A will be hyperbolic provided that $|\mathrm{tr}\, A| > 2$, which we assume from now on. A map of this form is called a (generalized) cat map and it represents the canonical example of an Anosov system [2].

A technical point to note is that in order to be able to quantize the maps we restrict A to be of one of the following forms:

$$A = \begin{pmatrix} \text{even} & \text{odd} \\ \text{odd} & \text{even} \end{pmatrix} \quad \text{or} \quad A = \begin{pmatrix} \text{odd} & \text{even} \\ \text{even} & \text{odd} \end{pmatrix}. \tag{5}$$

The classical dynamics of such automorphism of the torus possess strong arithmetic feature as a direct consequence of the linearity of the map. This, in particular, implies a linear structure for the stable and unstable manifolds and also a lattice-like structure for the periodic orbits that, in this case, coincides exactly with the set of rational points on $\mathbb{T}^2$. Elementary algebraic number theory constitutes a natural framework for the exploration of the classical properties of the map [27].

We will consider perturbations of this linear map by composing with a time $\kappa > 0$ flow of a global Hamiltonian $H(q, p)$ on $\mathbb{T}^2$.

Assume H to be a real function of the torus of the form

$$H(q, p) = \sum_{n,m\in\mathbb{Z}} a_{nm} \sin 2\pi(nq + mp) + b_{nm} \cos 2\pi(nq + mp),$$

with rapidly decaying coefficients a_{nm} and b_{nm}. Then, H induces a vector field $X_H = \left(\frac{\mathrm{d}H}{\mathrm{d}p}, -\frac{\mathrm{d}H}{\mathrm{d}q}\right)$ on $\mathbb{T}^2$ and a corresponding Hamiltonian flow $\phi_t : \mathbb{T}^2 \to \mathbb{T}^2$, $\phi_0(q, p) = (q, p)$. We now consider the time $t = \kappa > 0$ a perturbative parameter and let $A_\kappa := A \circ \phi_\kappa$.

It is known [1, 2] that there exists a $\kappa_{\max} > 0$, which depends on A and H, such that for values of $\kappa \in [0, \kappa_{\max})$, the map A_κ is still an Anosov map of the torus and moreover it is C^0-conjugate with the linear map A. Namely, for each κ fixed, there exists a continuous function Ψ_κ on $\mathbb{T}^2$ such that $\Psi_\kappa^{-1} \circ A \circ \Psi_\kappa = A_\kappa$. In particular, this implies that both the rigid spatial structure and the Lyapunov exponents of the periodic orbits can change drastically, but the global topological entropy remains constant.

In this paper, we consider the particular perturbations for which the Hamiltonian function H depends only on one coordinate. In this case, the corresponding Hamiltonian flow gives rise to non-linear shears. More precisely, assume, for example,

$$H(q) = \sum_{n\in\mathbb{Z}} a_n \sin(2\pi nq) + b_n \cos(2\pi nq).$$

It is then easy to see that the corresponding Hamiltonian flow at time κ is of the form

$$P_\kappa\begin{pmatrix} q \\ p \end{pmatrix} := \begin{pmatrix} q \\ p + \kappa f(q) \end{pmatrix}, \tag{6}$$

a shear in momentum, where

$$f(q) = -\frac{\mathrm{d}H}{\mathrm{d}q}.$$

Similarly, a Hamiltonian of the form

$$H(p) = \sum_{m\in\mathbb{Z}} a_m \sin(2\pi mp) + b_m \cos(2\pi mp)$$

generates a shear in position

$$Q_\kappa \begin{pmatrix} q \\ p \end{pmatrix} := \begin{pmatrix} q + \kappa g(p) \\ p \end{pmatrix}, \tag{7}$$

with $g(p) = \frac{\mathrm{d}H}{\mathrm{d}p}$.

We now turn to the quantum dynamics. As has been mentioned, the quantum propagator for the classical map A can be represented by an $N \times N$ matrix U. The components in the standard (position) basis can be written down explicitly in terms of the elements of A [19]. To be more precise, the form of the propagator also depends on the reduction of A_{12} and N by their greatest common divisor. We denote the reduced quantities $N' := N/\gcd(N, A_{12})$ and $A'_{12} := A_{12}/\gcd(N, A_{12})$. Then, for a cat map of the form (5), the kjth element of U is given by

$$U_{kj} = \left(\frac{A_{12}}{N}\right)^{1/2} \exp\left(\frac{\pi \mathrm{i}}{A_{12}N}(A_{11}j^2 - 2jk + A_{22}k^2)\right) G\left(N'A_{11}, A'_{12}, \frac{2(A_{11}j - k)}{\gcd(N, A_{12})}\right), \tag{8}$$

where G is a number-theoretical function related to Gauss averages. It is defined for coprime integers a and b by

$$G(a, b, c) := \lim_{M\to\infty} \frac{1}{2M} \sum_{m=-M}^{M} \exp\left(\frac{\pi \mathrm{i}}{b}(am^2 + cm)\right). \tag{9}$$

This function can be expressed in a closed form [19]. If $ab + c$ is not an even integer, then the average converges to 0. Otherwise,

$$G(a, b, c) = P(a, b)T(a, b, c), \tag{10}$$

where

$$P(a, b) := \begin{cases} \dfrac{1}{\sqrt{b}}\left(\dfrac{a}{b}\right) \exp\left(\dfrac{-\mathrm{i}\pi}{4}(b - 1)\right), & b \text{ odd}, \\ \dfrac{1}{\sqrt{b}}\left(\dfrac{b}{a}\right) \exp\left(\dfrac{\mathrm{i}\pi a}{4}\right), & b \text{ even}, \end{cases} \tag{11}$$

and

$$T(a, b, c) := \begin{cases} \exp\left(\dfrac{-\mathrm{i}\pi a}{b}(a\backslash b)^2(c/2)^2\right), & ab \text{ even}, \\ \exp\left(\dfrac{-4\mathrm{i}\pi a}{b}(4a\backslash b)^2c^2\right), & ab \text{ odd}. \end{cases} \tag{12}$$

In (11), only the notation $\left(\frac{a}{b}\right)$ premultiplying the exponential denotes the Jacobi symbol of number theory, although this function does not play any part in the following analysis; the notation $(a\backslash b)$ refers to the inverse of a modulo b—that is, the integer x such that $ax \equiv 1 \pmod{b}$. Since a and b are coprime, this is determined uniquely.

It is possible to quantize maps more general than those of the forms (5), if one introduces quantum boundary conditions [10, 22], but we do not consider this here.

The quantizations of the shears are easy to construct [4], since they are κ-time Hamiltonian flows. In the case of P_κ, for example, the quantum propagator $\hat{P}_\kappa$ is a diagonal matrix with

$$(\hat{P}_\kappa)_{kj} = \delta_{kj} \exp(2\pi \mathrm{i} N \kappa H(k/N)). \tag{13}$$

For the shear Q_κ in position, we can most easily construct the propagator by changing to momentum coordinates and finding a diagonal matrix in this representation. The change of basis matrix is the discrete Fourier transform $\mathcal{F}$, where

$$\mathcal{F}_{kj} := \frac{1}{\sqrt{N}} \exp\left(\frac{-2\pi \mathrm{i} kj}{N}\right).$$

The quantized shear in position is $\hat{Q}_\kappa$, where

$$\hat{Q}_\kappa = \mathcal{F}^{-1} D_\kappa \mathcal{F} \tag{14}$$

and D_κ is a diagonal matrix constructed as for $\hat{P}_\kappa$ above, this time looking for the $H = H(p)$ such that $g(p) = H'(p)$.

We denote again the composition of the map A with the two independent Hamiltonian flows by $A_{\boldsymbol{\kappa}}$, where $\boldsymbol{\kappa} := (\kappa_\mathrm{q}, \kappa_\mathrm{p})$ is the vector of strengths of the individual perturbations

$$A_{\boldsymbol{\kappa}} := A \circ P_{\kappa_\mathrm{p}} \circ Q_{\kappa_\mathrm{q}}$$

and the corresponding quantum propagator $V = V(A, \boldsymbol{\kappa}, f, g)$ is the product of the propagators of the individual maps

$$V = U \hat{P}_{\kappa_\mathrm{p}} \hat{Q}_{\kappa_\mathrm{q}}. \tag{15}$$

If we impose some more restrictions on the Fourier coefficients of H, we can gain some extra symmetries of the shears that, as we will see below, explain our numerical observations. In fact, note that if

$$H(q) = \sum_{r \in \mathbb{Z}} a_r \sin(2\pi(2r+1)q) + b_r \cos(4\pi r q), \tag{16}$$

then $H(q) = H\left(\frac{1}{2} - q\right)$, i.e. $f\left(\frac{1}{2} - q\right) = -f(q)$.

Our main results follow, to be proved in section 4. We describe certain circumstances for which operators commuting with V for a subset of values of N can be constructed. These operators are given explicitly in terms of their actions on the standard (position) basis vectors denoted as $\{\mathbf{e}_j\}_{j=0}^{N-1}$.

For brevity, we will often use the notation $e(x) := \mathrm{e}^{2\pi \mathrm{i} x}$ and $e_N(x) := e(x/N)$.

Theorem 1. *Let the shears P_{κ_p} and Q_{κ_q} be generated by Hamiltonians of the form (16) (for the Hamiltonian which generates Q_{κ_q} replace q by p in (16)). Then, if N is even, we can define an operator $\hat{W}$ by its action on the jth standard basis vector:*

$$\hat{W}\mathbf{e}_j := e(j/2)\mathbf{e}_{N/2-j}. \tag{17}$$

Then, if N is divisible by 4, $\forall \kappa_\mathrm{q}, \kappa_\mathrm{p} \geqslant 0$:

$$\hat{W}V = V\hat{W},$$

where $V = U\hat{P}_{\kappa_\mathrm{p}}\hat{Q}_{\kappa_\mathrm{q}}$.

Note that the conditions of theorem 1 place no restrictions on A other than that it be of the chessboard form (5).

We will also prove theorem 2, which for certain choices of A and only one perturbation in momentum, demonstrates the existence of some symmetries, without any restriction on the Hamiltonian generating P_κ.

Theorem 2. *Consider the unperturbed map A of the form (5) such that there exists an $s > 1$ with $s \mid \gcd(A_{12}, A_{22} - 1)$ if A_{12} is odd, or $2s \mid \gcd(A_{12}, A_{22} - 1)$ if A_{12} is even. Then, for $N = sM$ for any $M \in \mathbb{N}$ and any $1 \leqslant r < s$, the operator $\hat{R}_{r/s}$ commutes with $V = U\hat{P}_\kappa$ for any choice of function $H(q)$ generating P_κ and any $\kappa > 0$, where $\hat{R}_\beta$ acts by*

$$\hat{R}_\beta \mathbf{e}_j := e(\beta j)\mathbf{e}_j. \tag{18}$$

Before going into the proofs of the theorems, we first interpret the results.

3. Interpretations and explanation of the numerical results

We first point out that, assuming random matrix behaviour, theorem 1 explains the numerical pictures in figures 1 and 2. The Hamiltonian generating the shears in momentum in (1) and (2) is

$$H(q) = \frac{-1}{4\pi^2}\sin(2\pi q), \tag{19}$$

and for the shear in position in (2) the Hamiltonian is

$$H(p) = \frac{1}{4\pi^2}\sin(2\pi p). \tag{20}$$

Both (19) and (20) are members of the class (16). Theorem 1 implies that if N is divisible by 4, there exists a $\hat{W}$ which commutes with V, and hence they can be jointly diagonalized. Since $\hat{W}^2 = I$, the only eigenvalues of $\hat{W}$ are ± 1, and we can split the eigenvectors of V into two classes depending on how they transform under $\hat{W}$. These classes are independent and so if one looks at the spectrum as a whole, we see a superposition of two random matrix spectra for these values of N.

In general, one expects to see deviations from a single random matrix spectrum whenever there are extra symmetries of V, such as the examples constructed in theorems 1 and 2. The situation is analogous in quantum billiard problems to that where the billiard table has some symmetry, for example, a reflection symmetry (see, for example, [28]). In this case, the presence of symmetry would be obvious from the geometry of the problem. The fact that the examples we find only exist for a certain subset of values of N makes them noteworthy.

In examples where theorem 2 applies, the spectrum will decompose into s blocks, since the operator $\hat{R}_{r/s}$ is of order s. This explains the statistics observed in figure 3. The map (3) is such an example with $s = 13$, so the spectral statistics approach those of a superposition of 13 COE spectra and not Poisson statistics. Equation (A.12) indicates how the level spacing density of a large number of random matrix spectra approaches that of Poisson processes, so these two curves are very close (see figure A1), and are not distinguishable at the level of accuracy of the numerics in figure 3. So theorem 2 helps us to interpret the numerics correctly. In fact, we can find a choice of map A and values of N for which s can be arbitrarily large, i.e. the nearest-neighbour spacing density can be made arbitrarily close to the exponential density. Note, however, that we cannot use theorem 2 to produce a subsequence of N for which the nearest-neighbour density converges to the exponential density for a *fixed* map A.

We are able to offer a classical interpretation of the operators constructed in theorems 1 and 2. The operator $\hat{R}_{r/s}$ is a quantization of the simple translation of $\mathbb{T}^2$ given by

$$R_{r/s}\begin{pmatrix} q \\ p \end{pmatrix} := \begin{pmatrix} q \\ p + \frac{r}{s} \end{pmatrix}, \tag{21}$$

which is an exact quantization provided that $s \mid N$. For a detailed treatment of these translations, see [13, 25]. Clearly, $R_{r/s}$ commutes with P_κ for any choice of shear, and if $s \mid \gcd(A_{12}, A_{22}-1)$ it is easy to check that $R_{r/s}$ is a classical symmetry of A.

The map $\hat{W}$ in theorem 1 is a quantization of a composition of two translations, with inversion. Let

$$W\begin{pmatrix} q \\ p \end{pmatrix} := \begin{pmatrix} \frac{1}{2} - q \\ \frac{1}{2} - p \end{pmatrix}. \tag{22}$$

Then, for N even $\hat{W}$ is an exact quantization of W. For any chessboard (5) A, W is a symmetry, and for H satisfying (16), W is a symmetry of the generated shear in position, or momentum, and so it follows that W commutes with A_κ.

4. Proof of the main results

The heart of theorem 1 is the following proposition.

Proposition 3. *Let N be divisible by 4. Then, the matrix elements of U transform as*

$$e\left(\frac{j-k}{2}\right) U_{(N/2-k)(N/2-j)} = U_{kj}. \tag{23}$$

The proof of proposition 3 relies on a direct calculation, using elementary number theory, and it can be found in appendix B.

Proof of theorem 1. We prove that $\hat{W}$ commutes with each of the matrices multiplied in (15) to give V. The simplest to show is $\hat{P}_{\kappa_\mathrm{p}}$. We first observe that the inverse of $\hat{W}$ acts by

$$\hat{W}^{-1}\mathbf{e}_j = e\left(-\frac{1}{2}\left(\frac{N}{2} - j\right)\right)\mathbf{e}_{N/2-j}. \tag{24}$$

By assumption H satisfies

$$H(q) = H\left(\tfrac{1}{2} - q\right). \tag{25}$$

We consider the action on the jth basis vector.

$$\begin{aligned}
\hat{W}^{-1}\hat{P}_{\kappa_\mathrm{p}}\hat{W}\mathbf{e}_j &= e(j/2)\hat{W}^{-1}\hat{P}_{\kappa_\mathrm{p}}\mathbf{e}_{N/2-j} \\
&= e(j/2)e\left(N\kappa_\mathrm{p}H\left(\frac{1}{2} - \frac{j}{N}\right)\right)\hat{W}^{-1}\mathbf{e}_{N/2-j} \\
&= e\left(N\kappa_\mathrm{p}H\left(\frac{j}{N}\right)\right)\mathbf{e}_j, \quad \text{using (25)}, \\
&= \hat{P}_{\kappa_\mathrm{p}}\mathbf{e}_j,
\end{aligned} \tag{26}$$

proving that $\hat{W}^{-1}\hat{P}_{\kappa_\mathrm{p}}\hat{W} = \hat{P}_{\kappa_\mathrm{p}}$.

The proof that $\hat{W}$ commutes with U depends on proposition 3.

$$\begin{aligned}
\hat{W}^{-1}U\hat{W}\mathbf{e}_j &= e(j/2)\hat{W}^{-1}U\mathbf{e}_{N/2-j} \\
&= \sum_{r=0}^{N-1} e\left(\frac{j}{2}\right) U_{r,(N/2-j)}\hat{W}^{-1}\mathbf{e}_r \\
&= \sum_{r=0}^{N-1} e\left(\frac{j}{2} - \frac{1}{2}\left(\frac{N}{2} - r\right)\right) U_{r,(N/2-j)}\mathbf{e}_{N/2-r};
\end{aligned}$$

then we re-index the sum by substituting $k = N/2 - r$,

$$\begin{aligned} &= \sum_{k=0}^{N-1} e\left(\frac{j-k}{2}\right) U_{(N/2-k)(N/2-j)} \mathbf{e}_k \\ &= \sum_{k=0}^{N-1} U_{kj} \mathbf{e}_k, \quad \text{using proposition 3,} \\ &= U\mathbf{e}_j. \end{aligned} \tag{27}$$

Finally, we note that the discrete Fourier transform also transforms in the same way as U. That is,

$$\begin{aligned} \mathcal{F}_{(N/2-k)(N/2-j)} &= \frac{1}{\sqrt{N}} e_N\left(-\left(\frac{N}{2}-k\right)\left(\frac{N}{2}-j\right)\right) \\ &= \frac{1}{\sqrt{N}} e\left(-\frac{N}{4}+\frac{k+j}{2}\right) \mathcal{F}_{kj}. \end{aligned} \tag{28}$$

So, since N is divisible by 4, then $e\left(\frac{j-k}{2}\right)\mathcal{F}_{(N/2-k)(N/2-j)} = \mathcal{F}_{kj}$, and $\mathcal{F}$ commutes with $\hat{W}$ in a proof like the above. From (14) we see that this is enough to show that $\hat{W}$ commutes with $\hat{Q}_{\kappa_q}$, and hence finally with V. □

Proof of theorem 2. It is obvious that $\hat{R}_{r/s}$ commutes with $\hat{P}_\kappa$ since they are both represented by diagonal matrices.

To show that $\hat{R}_{r/s}$ commutes with the propagator of the unperturbed map U, we look at the matrix elements of $\hat{R}_{r/s}^{-1} U \hat{R}_{r/s}$; in the usual position basis, the kjth entry is

$$e\left(-\frac{r}{s}(k-j)\right) U_{kj}. \tag{29}$$

We will show that for every j, k either $U_{kj} = 0$ or $k \equiv j \pmod{s}$, thereby proving that $\hat{R}_{r/s}^{-1} U \hat{R}_{r/s} = U$.

If $U_{kj} \neq 0$, then we must have that the third argument of the function G in (8) is an integer, say $\frac{2(A_{11}j-k)}{\gcd(N,A_{12})} = m$. Rearranging we get

$$k - j = (A_{11} - 1)j - \frac{m}{2}\gcd(N, A_{12}). \tag{30}$$

We show that s divides both terms on the right-hand side of (30). Since $s \mid A_{12}$, it follows from $A_{11}A_{22} - A_{12}A_{21} = 1$ that

$$A_{11}A_{22} \equiv 1 \pmod{s}. \tag{31}$$

Also, since $s \mid (A_{22} - 1)$, we have

$$A_{22} \equiv 1 \pmod{s}. \tag{32}$$

Subtracting (32) from (31), we get

$$(A_{11} - 1)A_{22} \equiv 0 \pmod{s}, \tag{33}$$

but s and A_{22} are coprime so we must have $s \mid (A_{11} - 1)$.

If $N'A_{11}A'_{12}$ is even, then m is even, so that to finish we need only show that $s \mid \gcd(N, A_{12})$. This follows from the assumptions that $s \mid A_{12}$ and $s \mid N$.

On the other hand, if $N'A_{11}A'_{12}$ is odd, then m is odd and we need to show that $s \mid \gcd(N, A_{12})/2$. By assumption $s \mid A_{12}/2$, and since A_{12} and N contain exactly the same power of 2 in their prime factorizations (we know this because $N'A'_{12}$ is odd), $s \mid N$ implies that $s \mid N/2$.

So, in all cases, $s \left| \frac{m}{2} \right. \gcd(N, A_{12})$ and we are done. □

5. Conclusions

In this paper, we have described how certain classical symmetries for the perturbed cat maps can be quantized to give quantum symmetries for certain values of the inverse Planck constant N and effect the spectral statistics of the quantum model.

The symmetries we have constructed are unrelated to the Hecke operators previously studied [21, 24] which have *no* classical interpretation. Our symmetries have a very simple classical origin and were first noted in [21]. In fact, classical symmetries of these types are very numerous for the unperturbed map A. One can replace the point $\left(\frac{1}{2}, \frac{1}{2}\right)$ in (22) with any fixed point of A. If the Hamiltonians are chosen so that the shears commute with this new map, then there will be, for certain values of N, a corresponding quantum symmetry. That $\hat{W}$ is a symmetry for every quantizable cat map (for the correct choices of N) is because $\left(\frac{1}{2}, \frac{1}{2}\right)$ is a fixed point of every chessboard map (5).

We mention that our results do not depend on the perturbation strength κ. Indeed, extending κ far beyond $\kappa_{\max}$, we still see the same spectral behaviour, even if this is somewhat unphysical because the perturbed map is then no longer conjugate to the unperturbed one.

We finally mention the implications of these results for a semi-classical theory of spectral fluctuations for these systems, which is one goal of current research in quantum chaology.

In the explicit examples we have given and in the possible other examples mentioned above, we have explained how certain subsequences of N can give spectral statistics different to those along the *main* subsequence. Any semi-classical theory for these maps must therefore not only predict the behaviour along the main subsequence—which (conjecturally) is convergence to a single random matrix spectrum of the correct universality class—but also the limits along the subsequences for which extra symmetry exists. Alternatively, to avoid these symmetries, one must restrict attention to subsequences avoiding values of N for which these symmetries are present. But this set has a positive density (at least $1/4$). Since the symmetries we have constructed can only exist for composite values of N, in order to be *completely* sure of avoiding them, it would be necessary to consider the $N \to \infty$ limit along N which are prime numbers, a density zero set of N.

Alternatively, to look for convergence along the full set of $N \in \mathbb{N}$ in future analytical studies, the perturbation and the unperturbed map should be chosen so that none of the symmetries found are present. In this case, it should be noted that (16) gives a non-small class of perturbations to avoid, in particular it includes the simplest and most common perturbation used in applications, that given by (19). Also, the simplest perturbation to perform is a single shear in momentum. But theorem 2 then places a restriction on the matrices A that should be used, since the symmetry $\hat{R}_{r/s}$ will commute with *any* shear in momentum.

Figure 3 illustrates the dangers of misleading numerics in the presence of a considerable number of symmetries.

Our results do not contradict the random matrix conjecture, but they do reveal further complications in the search for a semi-classical theory of spectral statistics of perturbed cat maps. The effects at the level of the spectral form factor will form the basis of a forthcoming work [14].

Acknowledgments

We are very grateful to Sandro Graffi, Jon Keating, Pär Kurlberg and Francesco Mezzadri for helpful ideas and comments.

Appendix A. Nearest-neighbour distribution

In this appendix, we briefly describe one of the most common spectral statistics used to measure the correlations of quantum spectra.

We assume that we have a sequence of real numbers, which we sometimes call levels $(\lambda_j)_{j=1}^{\infty}$, ordered so that $0 \leqslant \lambda_1 \leqslant \lambda_2 \leqslant \cdots$, and mean spacing ρ^{-1}, that is,

$$\lim_{N\to\infty} \frac{\#\{j : \lambda_j < N\}}{N} = \rho. \tag{A.1}$$

In order to compare different sequences (λ_j), we first 'standardize' them by rescaling so that $\rho = 1$. Then, a typical quantity to investigate is the nearest-neighbour spacing density $P(s)$ which is defined by

$$\lim_{N\to\infty} \frac{1}{N} \sum_{j=1}^{N} h(\lambda_{j+1} - \lambda_j) = \int_0^{\infty} h(s) P(s)\, \mathrm{d}s, \tag{A.2}$$

if such a $P(s)$ exists for some class of test functions $h(s)$.

Usually, we compare the sequence of normalized levels of a quantum spectrum with a sequence of eigenvalues of an ensemble of random matrices. In this case, the quantity $P(s)$ is averaged with respect to the probability measure of the ensemble before the limit $N \to \infty$ is taken. The closed forms of the nearest-neighbour density for ensembles of random matrices can be given in terms of Painlevé functions [16], but for numerical studies, the Wigner surmises give a good numerical approximation. For the circular orthogonal ensemble, it reads

$$P^{\mathrm{COE}}(s) \approx \frac{\pi s}{2} \mathrm{e}^{-\pi s^2/4}, \tag{A.3}$$

and for the circular unitary ensemble,

$$P^{\mathrm{CUE}}(s) \approx \frac{32 s^2}{\pi^2} \mathrm{e}^{-4s^2/\pi}. \tag{A.4}$$

If the points λ_j are ordered event times of a Poisson process—so completely uncorrelated—then the nearest-neighbour spacings are exponentially distributed (see e.g. [15], section I.4);

$$P^{\mathrm{Poisson}}(s) = \mathrm{e}^{-s}. \tag{A.5}$$

A.1. Nearest-neighbour spacing density for a superposition of independent spectra

We now consider the case where the sequence (λ_j) is formed by superimposing n independent sets of points with the same given spectral statistics, where the fraction of levels coming from the kth component in the superposition is ρ_k. This means that the mean level spacing of this component considered in isolation is ρ_k^{-1}.

Denote by $P(s)$ the nearest-neighbour spacing density of the superimposed spectrum, scaled to have mean spacing 1, and by $P^n(s)$ the density for the resulting spectrum. In what follows, we implicitly assume that $P(s)$ can be represented by a bounded function, decaying rapidly as $s \to \infty$. This is certainly the case for random matrix ensembles. A formula for $P^n(s)$ in terms of $P(s)$ appears to have been first given in the appendix to [30]. An alternative argument leading to the same formula is given in appendix A.2 of [26].

Given

$$E(s) := \int_0^{\infty} x P(x+s)\, \mathrm{d}x, \tag{A.6}$$

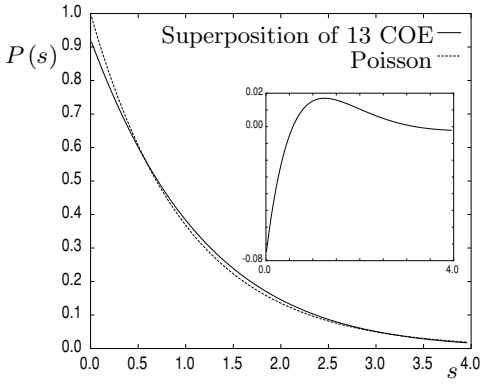

Figure A1. A comparison of the nearest-neighbour distribution for a superposition of 13 independent COE spectra, and the exponential density for Poisson events. Inset: the difference $P^{\mathrm{COE},13}(s) - P^{\mathrm{Poisson}}(s)$.

Then, $P^n(s)$ is given by

$$P^n(s) = \Pi(s)\left(\sum_{k=1}^{n}\rho_k^2\left(\frac{P(\rho_k s)}{E(\rho_k s)} - \frac{E'(\rho_k s)^2}{E(\rho_k s)^2}\right) + \left(\sum_{k=1}^{n}\rho_k\frac{E'(\rho_k s)}{E(\rho_k s)}\right)^2\right), \tag{A.7}$$

where

$$\Pi(s) := \prod_{k=1}^{n} E(\rho_k s). \tag{A.8}$$

As an example, for a superposition of two equally weighted spectra, we have

$$P^2(s) = \frac{1}{2}P\left(\frac{s}{2}\right)E\left(\frac{s}{2}\right) + \frac{1}{2}E'\left(\frac{s}{2}\right)^2. \tag{A.9}$$

We can get approximations to the spectral statistics of a superimposition of two COE (resp. CUE) sequences by substituting the Wigner surmise (A.3) (resp. (A.4)) into (A.9). We find, using (A.6),

$$E^{\mathrm{COE}}(s) \approx 1 - \mathrm{erf}\left(\frac{s\sqrt{\pi}}{2}\right) \tag{A.10}$$

and

$$E^{\mathrm{CUE}}(s) \approx \mathrm{e}^{-4s^2/\pi} + s\,\mathrm{erf}\left(\frac{2s}{\sqrt{\pi}}\right) - s. \tag{A.11}$$

Substituting (A.10) and (A.11) into (A.9) gives the functions plotted as the curves in the plots on the right in figures 1 and 2.

In the case when all ρ_k are equal to $1/n$, it is shown in [26, 30] that

$$\lim_{n\to\infty} P^n(s) = \mathrm{e}^{-s}. \tag{A.12}$$

The intuitive explanation is quite simple: in a superposition of a very large number of independent sequences, with high probability a given level and its neighbour will be from different sequences, so the behaviour would be expected to be the same as for uncorrelated levels (cf equation (A.5)). The rate of convergence is fast enough that even for relatively low n, the difference between the superimposed spectra and Poisson can be difficult to distinguish by eye. As an illustration, we present figure A1 which shows an example with $n = 13$.

Appendix B. Proof of proposition 3

The proof of proposition 3 is elementary, but rather long. It is split into two parts, depending on the parity of the product $N'A_{11}A'_{12}$. For the most part, the proof involves repeated use of the identity

$$A_{11}A_{22} - A_{12}A_{21} = 1, \tag{B.1}$$

to reduce resulting expressions. Note that (B.1) implies that A_{11} (and A_{22}) is coprime to A_{12}.

Proof of proposition 3. To simplify we rewrite for fixed A and N,

$$U_{kj} = \tilde{P}E(k, j)g(k, j), \tag{B.2}$$

where the prefactor $\tilde{P}$ contains all the factors that do not depend on j, k, and

$$E(k, j) := e\left(\frac{1}{2NA_{12}}(A_{11}j^2 - 2jk + A_{22}k^2)\right) \tag{B.3}$$

and

$$g(k, j) := T\left(N'A_{11}, A'_{12}, \frac{2(A_{11}j - k)}{\gcd(N, A_{12})}\right). \tag{B.4}$$

We first assume that $N'A_{11}A'_{12}$ is even. Then, we only need consider those j, k for which $\frac{2(A_{11}j-k)}{\gcd(N,A_{12})}$ is an even integer. To see this note that if it is not an even integer then $g(k, j) = 0$, and we need only to check that this is inherited when we replace k and j with $N/2 - k$ and $N/2 - j$. Making this substitution,

$$\frac{2}{\gcd(N, A_{12})}\left(A_{11}\left(\frac{N}{2} - j\right) - \left(\frac{N}{2} - k\right)\right) = \frac{N(A_{11} - 1)}{\gcd(N, A_{12})} - \frac{2(A_{11}j - k)}{\gcd(N, A_{12})}. \tag{B.5}$$

If A_{12} is even, then $A_{11} - 1$ is even, and oddity is preserved by the transformation (B.5), giving $g(N/2 - k, N/2 - j) = 0$. On the other hand, if A_{12} is odd, then $2 \nmid \gcd(N, A_{12})$ and if $\frac{2(A_{11}j-k)}{\gcd(N,A_{12})}$ is not even, then it is not an integer (we obviously only need to consider the case $\gcd(N, A_{12}) > 1$), so here we also have $g(k, j) = 0$.

From (B.3), we easily get

$$e\left(\frac{j - k}{2}\right)E\left(\frac{N}{2} - k, \frac{N}{2} - j\right) = E(k, j)e\left((-A_{11} + A_{12} + 1)\frac{j}{2A_{12}} + \frac{A_{11} + A_{22} - 2}{8A_{12}}N + (-A_{22} - A_{12} + 1)\frac{k}{2A_{12}}\right). \tag{B.6}$$

Then, we write $k = A_{11}j - C\gcd(N, A_{12})$ for some $C \in \mathbb{Z}$. After doing this, and using (B.1) several times, we get

$$\begin{aligned} e\left(\frac{j - k}{2}\right)E\left(\frac{N}{2} - k, \frac{N}{2} - j\right) &= E(k, j)e\left((A_{12} + 1 - A_{11}A_{22} - A_{11}A_{12})\frac{j}{2A_{12}} + \frac{A_{11} + A_{22} - 2}{8A_{12}}N - (-A_{22} - A_{12} + 1)\frac{C}{2A'_{12}}\right) \\ &= E(k, j)e\left(A_{12}(1 - A_{21} - A_{11})\frac{j}{2A_{12}} + \frac{A_{11} + A_{22} - 2}{8A_{12}}N - (-A_{22} - A_{12} + 1)\frac{C}{2A'_{12}}\right), \end{aligned}$$

using $A_{11}A_{22} - A_{21}A_{12} = 1$,

$$= E(k, j)e\left(\frac{A_{11} + A_{22} - 2}{8A_{12}}N + (A_{22} + A_{12} - 1)\frac{C}{2A'_{12}}\right). \tag{B.7}$$

We now look at how g transforms. Denoting again $k = A_{11}j - C\gcd(N, A_{12})$, then

$$g(k, j) = e\left(\frac{-N'A_{11}}{2A'_{12}}(N'A_{11}\backslash A'_{12})^2C^2\right), \tag{B.8}$$

and using (B.5),

$$\begin{aligned} g\left(\frac{N}{2} - k, \frac{N}{2} - j\right) &= g(k, j)e\left(\frac{-N'A_{11}}{2A'_{12}}(N'A_{11}\backslash A'_{12})^2\frac{N'(A_{11} - 1)}{2}\left(\frac{N'(A_{11} - 1)}{2} - 2C\right)\right) \\ &= g(k, j)e\left(\frac{-N'A_{11}}{2A'_{12}}(N'A_{11}\backslash A'_{12})^2\left(\frac{N'(A_{11} - 1)}{2}\right)^2\right) \\ &\quad \times e\left(\frac{N'A_{11}}{2A'_{12}}(N'A_{11}\backslash A'_{12})^2N'(A_{11} - 1)C\right). \end{aligned} \tag{B.9}$$

We simplify by noting that $N'(N'A_{11}\backslash A'_{12}) \equiv A_{22} \pmod{A'_{12}}$. In fact, let $y = N'(N'A_{11}\backslash A'_{12})$. Then,

$$A_{11}y \equiv 1 \pmod{A'_{12}} \tag{B.10}$$

by definition. But also, from (B.1),

$$\begin{aligned} A_{11}A_{22} &= 1 + A_{21}\gcd(N, A_{12})A'_{12} \\ &\equiv 1 \pmod{A'_{12}}. \end{aligned} \tag{B.11}$$

Subtracting gives

$$A_{11}(y - A_{22}) \equiv 0 \pmod{A'_{12}}, \tag{B.12}$$

and since A_{11} and A'_{12} are coprime, then $A'_{12} \mid (y - A_{22})$.

Thus, we have, for some $m \in \mathbb{Z}$,

$$\begin{aligned} e\left(\frac{N'A_{11}}{2A'_{12}}(N'A_{11}\backslash A'_{12})^2N'(A_{11} - 1)C\right) &= e\left(\frac{A_{11}(A_{11} - 1)}{2A'_{12}}(A_{22} + mA'_{12})^2C\right) \\ &= e\left(\frac{A_{11}(A_{11} - 1)}{2A'_{12}}A_{22}^2C\right), \end{aligned}$$

using the fact that $A_{11}(A_{11} - 1)$ is even,

$$\begin{aligned} &= e\left(\frac{(1 + A_{12}A_{21})(A_{11} - 1)}{2A'_{12}}A_{22}C\right) \\ &= e\left(\frac{(A_{11} - 1)A_{22}}{2A'_{12}}C\right), \end{aligned}$$

using the fact that $A_{22}(A_{11} - 1)$ is even,

$$= e\left(\frac{1 + A_{12}A_{21} - A_{22}}{2A'_{12}}C\right). \tag{B.13}$$

We can similarly treat

$$e\left(\frac{-N'A_{11}}{8A'_{12}}N'^2(N'A_{11}\backslash A'_{12})^2(A_{11}-1)^2\right) = e\left(\frac{-NA_{11}}{8A_{12}}(A_{22}+mA'_{12})^2(A_{11}-1)^2\right)$$
$$= e\left(\frac{-NA_{11}}{8A_{12}}(A_{11}A_{22}-A_{22}+mA'_{12}(A_{11}-1))^2\right)$$
$$= e\left(\frac{-NA_{11}}{8A_{12}}((1-A_{22})^2+\ell A'_{12})\right) \tag{B.14}$$

where, after inserting (B.1), ℓ is the integer defined by

$$(1-A_{22}+A_{12}A_{21}+mA'_{12}(A_{11}-1))^2 =: (1-A_{22})^2+\ell A'_{12}. \tag{B.15}$$

If A_{11} is even, then $4 \nmid \gcd(N, A_{12})$, so using the assumption that $4 \mid N$, we see that the term involving ℓ disappears from (B.14). If A_{11} is odd, then this term will still vanish provided we can be sure that

$$\frac{N'm^2{A'_{12}}^2(A_{11}-1)^2}{8A'_{12}} \in \mathbb{Z}. \tag{B.16}$$

But since $(A_{11}-1)$ is even, and we are in the regime $N'A_{11}A'_{12}$ even, then this follows immediately. So, following (B.14), we have that

$$e\left(\frac{-N'A_{11}}{8A'_{12}}N'^2(N'A_{11}\backslash A'_{12})^2(A_{11}-1)^2\right) = e\left(\frac{-NA_{11}}{8A_{12}}\left(1-2A_{22}+A_{22}^2\right)\right)$$
$$= e\left(\frac{-N}{8A_{12}}(A_{11}-(2-A_{22})(1+A_{21}A_{12}))\right)$$
$$= e\left(\frac{-N}{8A_{12}}(A_{11}+A_{22}-2-(2-A_{22})A_{12}A_{21})\right)$$
$$= e\left(\frac{-N}{8A_{12}}(A_{11}+A_{22}-2)\right), \tag{B.17}$$

since $(2-A_{22})A_{21}$ is even, and $4|N$.

Finally, collecting together (B.7), (B.9), (B.13) and (B.17) and substituting into (23), after some cancellations we get

$$e\left(\frac{j-k}{2}\right)U_{N/2-k,N/2-j} = e\left(\frac{A_{12}(1+A_{21})}{2A'_{12}}C\right)U_{kj}$$
$$= e\left(\frac{\gcd(N,A_{12})(1+A_{21})}{2}C\right)U_{kj}$$
$$= U_{kj}, \tag{B.18}$$

where the last line follows since either A_{21} is odd, or otherwise $2 \mid \gcd(A_{12}, N)$.

We now consider the case where $N'A_{11}A'_{12}$ is odd. Note that this implies A_{11} is odd. Since the chessboard form gives that A_{12} then must be even, for A'_{12} to then be odd implies that $2 \mid \gcd(N, A_{12})$.

As before, (B.6) holds. But now we need to consider $\frac{2(A_{11}j-k)}{\gcd(N,A_{12})}$ odd. Otherwise $g(k, j) = 0$, and since the first term on the right-hand side of (B.5) is even, also $g(N/2-k, N/2-j) = 0$. So we can assume that

$$k = A_{11}j - \frac{L}{2}\gcd(N, A_{12}), \tag{B.19}$$

for some odd $L \in \mathbb{Z}$. Substituting into (B.6) yields

$$e\left(\frac{j-k}{2}\right) E\left(\frac{N}{2}-k, \frac{N}{2}-j\right) = E(k,j)e\left(\frac{A_{11}+A_{22}-2}{8A_{12}}N + (A_{22}+A_{12}-1)\frac{L}{4A'_{12}}\right). \tag{B.20}$$

In this regime we have the second form of T given in (12), so

$$\begin{aligned} g\left(\frac{N}{2}-k, \frac{N}{2}-j\right) &= e\left(\frac{-2N'A_{11}}{A'_{12}}(4N'A_{11}\backslash A'_{12})^2(N'(A_{11}-1)-L)^2\right) \\ &= g(k,j)e\left(\frac{-2N'A_{11}}{A'_{12}}N'^2(4N'A_{11}\backslash A'_{12})^2(A_{11}-1)^2\right) \\ &\quad \times e\left(\frac{4A_{11}(A_{11}-1)}{A'_{12}}N'^2L(4N'A_{11}\backslash A'_{12})^2\right). \end{aligned} \tag{B.21}$$

Again, we simplify, noting that

$$\begin{aligned} 4N'(4N'A_{11}\backslash A'_{12}) &\equiv A_{22} \pmod{A'_{12}} \\ &= A_{22} + mA'_{12} \end{aligned} \tag{B.22}$$

for some m. In fact, m must be odd, because both A_{22} and A'_{12} are odd. So,

$$\begin{aligned} e\left(\frac{4A_{11}(A_{11}-1)}{A'_{12}}N'^2L(4N'A_{11}\backslash A'_{12})^2\right) &= e\left(\frac{A_{11}(A_{11}-1)}{4A'_{12}}L(A_{22}+mA'_{12})^2\right) \\ &= e\left(\frac{A_{11}(A_{11}-1)}{4A'_{12}}L\left(A_{22}^2+m^2A'^2_{12}\right)\right) \\ &= e\left(\frac{A_{11}(A_{11}-1)}{4A'_{12}}LA_{22}^2 + \frac{A_{11}-1}{4}\right), \end{aligned} \tag{B.23}$$

where the last line follows because all of A_{11}, m, L and A'_{12} are odd. It now follows through repeated use of (B.1) that

$$e\left(\frac{-4A_{11}(A_{11}-1)}{A'_{12}}N'^2L(4N'A_{11}\backslash A'_{12})^2\right) = e\left(\frac{1+A_{12}A_{21}-A_{22}}{4A'_{12}}L\right)e\left(\frac{A_{11}-1}{4}\right). \tag{B.24}$$

Also,

$$\begin{aligned} e\left(\frac{-2N'A_{11}}{A'_{12}}N'^2(4N'A_{11}\backslash A'_{12})^2(A_{11}-1)^2\right) &= e\left(\frac{-N'A_{11}}{8A'_{12}}(A_{22}+mA'_{12})^2(A_{11}-1)^2\right) \\ &= e\left(\frac{-N'A_{11}}{8A'_{12}}(A_{11}-1)^2A_{22}^2 - \frac{(A_{11}-1)^2}{8}\right) \\ &= e\left(\frac{-N'A_{11}}{8A'_{12}}(1-A_{22}+A_{12}A_{21})^2 - \frac{(A_{11}-1)^2}{8}\right) \\ &= e\left(\frac{-N'A_{11}}{8A'_{12}}(1-A_{22})^2 - \frac{(A_{11}-1)^2}{8}\right) \\ &= e\left(-\frac{N(A_{11}+A_{22}-2)}{8A_{12}}\right)e\left(-\frac{(A_{11}-1)^2}{8}\right), \end{aligned} \tag{B.25}$$

Collecting together (B.20), (B.21), (B.24) and (B.25), we get

$$\begin{aligned} e\left(\frac{j-k}{2}\right)U_{(N/2-k),(N/2-j)} &= U_{kj}e\left(-\frac{(A_{11}-1)^2}{8}\right)e\left(\frac{A_{12}(1+A_{21})}{4A'_{12}}L\right)e\left(\frac{A_{11}-1}{4}\right) \\ &= U_{kj}e\left(-\frac{(A_{11}-1)(A_{11}-3)}{8}\right)e\left(\frac{\gcd(N,A_{12})}{4}\right). \end{aligned} \tag{B.26}$$

We now note that precisely one of $A_{11} - 1$ and $A_{11} - 3$ is divisible by 4 and the other divisible by 2, cancelling 8 in the denominator of the first exponential on the right-hand side of (B.26). If $4 \mid N$, and N' is odd, then we must have $4 \mid \gcd(N, A_{12})$, so the factor on the right-hand side of (B.26) is unity, and we are done. □

References

[1] Anosov D V 1962 Roughness of geodesic flows on compact Riemannian manifolds of negative curvature *Dokl. Akad. Nauk SSSR* **145** 707–9

[2] Arnol'd V I and Avez A 1967 *Problemes Ergodiques de la Mecanique Classique* (Paris: Gauthier-Villars)

[3] Bäcker A 2003 Numerical aspects of eigenvalue and eigenfunction computations for chaotic quantum systems *The Mathematical Aspects of Quantum Maps (Lecture Notes in Physics* vol 618*)* ed M Degli Esposti and S Graffi (Berlin: Springer)

[4] Basilio de Matos M and Ozorio de Almeida A M 1995 Quantization of Anosov maps *Ann. Phys.* **237** 46–65

[5] Berry M V and Robnik M 1986 Statistics of energy levels without time-reversal symmetry: Aharonov–Bohm chaotic billiards *J. Phys. A: Math. Gen.* **19** 649–68

[6] Berry M V and Tabor M 1977 Level clustering in the regular spectrum *Proc. R. Soc. Lond.* A **356** 375–94

[7] Bogomolny E B, Georgeot B, Giannoni M-J and Schmit C 1997 Arithmetical chaos *Phys. Rep.* **291** 219–324

[8] Bohigas O, Giannoni M-J and Schmit C 1984 Characterization of chaotic quantum spectra and universality of level fluctuation laws *Phys. Rev. Lett.* **52** 1–4

[9] Casati G, Valz-Griz F and Guarneri I 1980 On the connection between the quantization of nonintegrable systems and statistical theory of spectra *Lett. Nuovo Cimento* **28** 279–82

[10] Degli Esposti M 1993 Quantization of the orientation preserving automorphisms of the torus *Ann. Inst. Henri Poincaré* **58** 323–41

[11] Degli Esposti M and Graffi S (ed) 2003 *The Mathematical Aspects of Quantum Maps (Lecture Notes in Physics* vol 618*)* (Berlin: Springer)

[12] Degli Esposti M and Graffi S (ed) 2003 *The Mathematical Aspects of Quantum Maps (Lecture Notes in Physics* vol 618*)* (Berlin: Springer) pp 49–90

[13] Degli Esposti M, O'Keefe S and Winn B 2005 A semi-classical study of the Casati–Prosen triangle map *Nonlinearity* **18** 1073–94

[14] Degli Esposti M and Winn B work in progress

[15] Feller W 1971 *An Introduction to Probability Theory and its Applications* vol 2 (New York: Wiley)

[16] Forrester P J and Witte N S 2000 Exact Wigner surmise type evaluation of the spacing distribution in the bulk of the scaled random matrix ensembles *Lett. Math. Phys.* **53** 195–200

[17] Guhr T, Müller-Groeling A and Weidenmüller H A 1998 Random-matrix theories in quantum physics: common concepts *Phys. Rep.* **299** 189–425

[18] Giraud O, Marklof J and O'Keefe S 2005 Intermediate statistics in quantum maps *J. Phys. A: Math. Gen.* **37** L303–11

[19] Hannay J H and Berry M V 1980 Quantization of linear maps on the torus—Fresnel diffraction by a periodic grating *Physica* D **1** 267–90

[20] Keating J P 1991 The cat maps: quantum mechanics and classical motion *Nonlinearity* **4** 277–307

[21] Keating J P and Mezzadri F 2000 Pseudo-symmetries of Anosov maps and spectral statistics *Nonlinearity* **13** 747–75

[22] Keating J P, Mezzadri F and Robbins J M 1999 Quantum boundary conditions for torus maps *Nonlinearity* **12** 579–91

[23] Kottos T and Smilansky U 1999 Periodic orbit theory and spectral statistics for quantum graphs *Ann. Phys.* **274** 76–124

[24] Kurlberg P and Rudnick Z 2000 Hecke theory and equidistribution for the quantization of linear maps of the torus *Duke Math. J.* **103** 47–77

[25] Marklof J and Rudnick Z 2000 Quantum unique ergodicity for parabolic maps *Geom. Funct. Anal.* **10** 1554–78

[26] Mehta M L 1991 *Random Matrices* (New York: Academic)

[27] Percival I and Vivaldi F 1987 Arithmetical properties of strongly chaotic motions *Physica* D **25** 105–30

[28] Sieber M and Steiner F 1990 Quantum chaos in the hyperbola billiard *Phys. Lett.* A **148** 415–20

[29] Robnik M 1986 Antiunitary symmetries and energy level statistics *Quantum Chaos and Statistical Nuclear Physics (Lecture Notes in Physics* vol 263*)* ed T H Seligman and H Nishioka (Berlin: Springer) pp 120–30

[30] Rosenzweig N and Porter C E 1960 'Repulsion of energy levels' in complex atomic spectra *Phys. Rev.* **120** 1698–714